



# Removal of hydrogen sulfide using crushed oyster shell from pore water to remediate organically enriched coastal marine sediments

Asaoka, Satoshi  
Yamamoto, Tamiji  
Kondo, Shunsuke  
Hayakawa, Shinjiro

---

## (Citation)

Bioresource Technology, 100(18):4127-4132

## (Issue Date)

2009-09

## (Resource Type)

journal article

## (Version)

Accepted Manuscript

## (Rights)

©2009 Elsevier.

This manuscript version is made available under the CC-BY-NC-ND 4.0 license  
<http://creativecommons.org/licenses/by-nc-nd/4.0/>

## (URL)

<https://hdl.handle.net/20.500.14094/90003333>



1 Removal of hydrogen sulfide using crushed oyster shell from pore water to  
2 remediate organically enriched coastal marine sediments

3  
4 Satoshi Asaoka<sup>a</sup>, Tamiji Yamamoto<sup>a\*</sup>, Shunsuke Kondo<sup>a</sup>, Shinjiro Hayakawa<sup>b</sup>

5 a) Graduate School of Biosphere Science, Hiroshima University

6 1-4-4 Kagamiyama, Higashi-Hiroshima, Japan 739-8528

7  
8 b) Graduate School of Engineering, Hiroshima University

9 1-4-1 Kagamiyama, Higashi-Hiroshima, Japan 739-8527

10  
11  
12 \*Corresponding author

13 Tel: +81-82-424-7945

14 Fax: +81-82-424-7998

15 E-mail address: tamiyama@hiroshima-u.ac.jp

16 Address: Graduate School of Biosphere Science, Hiroshima University

17 1-4-4 Kagamiyama, Higashi-Hiroshima, Japan 739-8528

## Abstract

Hydrogen sulfide is highly toxic and fatal to benthic organisms as well as causing depletion of dissolved oxygen and generating blue tide in eutrophic coastal seas. The purposes of this study are to reveal adsorption characteristics of hydrogen sulfide onto crushed oyster shell, and to evaluate removal efficiency of hydrogen sulfide from pore water in organically enriched sediments using container experiment in order to develop a coastal sediment amendment. The crushed oyster shell was mainly composed of  $\text{CaCO}_3$  with calcite and CaO crystal phase. The batch experiment showed removal kinetics of hydrogen sulfide can be expressed as the first order equation and Langmuir plot fitted well in describing the adsorption behavior with the adsorption maximum at  $12 \text{ mg-S g}^{-1}$ . The container experiments suggested the oyster shell adsorbs hydrogen sulfide in pore water effectively and reduces oxygen consumption in the overlying water. Furthermore, oxidation-reduction potential of the sediment was higher with addition of crushed oyster shell than the control without oyster shell. Thus, it is concluded that crushed oyster shell can be an effective amendment to remediate organically enriched sediments in eutrophic coastal seas.

## Key words

adsorption, enclosed water body, hydrogen sulfide, sediment, ORP

## 1. Introduction

Hydrogen sulfide is a byproduct of sulfate reduction that is highly toxic to benthic organisms in enclosed or semi-enclosed coastal seas. Sulfate reduction is followed by oxygen depletion due to decomposition of organic matter and the resulting hydrogen sulfide sometimes generates blue tide when it is oxidized at the sea surface. Sediments of coastal area that are highly influenced by human activity contain a high much amount of organic matter, which can be a major cause of the formation of hydrogen sulfide.

In Japan, 200 G g of oysters were produced in 2007 and more than half come from Hiroshima prefecture (Ministry of Agriculture, Forestry and Fisheries of Japan, 2007). The intensive oyster culture in Hiroshima Bay causes accumulation of organic matter on the sediment, resulting into high hydrogen sulfide levels. Oyster meat themselves is consumed and a significant amount of oyster shell is discarded. Some oyster shells are reused as soil conditioners and feeds for chicken, while others are left piling up in the field producing unpleasant fishy smell for a long period. Therefore, new applications utilizing these discarded oyster shells are expected to contribute towards promoting recycling consciousness within the society.

While several studies have been carried out for other applications of oyster shell as filtering medium (Park and Polprasert, 2008), catalyst (Nakatani et al., 2009), construction material (Yoon et al., 2003) and soil conditioner (Lee et al., 2008ab), there is few information on the application of crushed oyster shells for the removal of hydrogen sulfide from pore water in order to remediate coastal marine sediments. Since the sediments within the oyster culture grounds are rich in organic matter, using crushed oyster shells to remove the hydrogen sulfide from the sediment will be consistent with the objectives of recycling and environmental restoration.

The purposes of the this study are (1) to determine some adsorption characteristics of hydrogen sulfide onto crushed oyster shells, and (2) to evaluate the removal efficiency of hydrogen sulfide from pore water in organically enriched sediments.

## **2. Materials and methods**

### **2.1. Characterization of crushed oyster shells**

The crushed oyster shells called "Matsu" used in this study were provided by Maruei Corporation, Hiroshima, Japan. They had been left soaking in seawater for 1~2 years to remove any remnants of oyster meat and dried in the field for 3~4 months to remove moisture and salts. The oyster shells were then crushed into coarse pieces and dried in an oven at 400 °C until the water contents falls below 6~7%. Finally, the coarse pieces were further crushed into 7~12 mm pieces. They are sold as feeds for chicken in Japan. It is not difficult to obtain a lot of crushed oyster shells with 7~12 mm pieces to remediate coastal sediment because some mass production plants for the materials are already in operation. The previous study on the material applied for soil conditioner showed that the more crushed or smaller the pieces are, the higher the soil pH increase due to calcium dissolution (Yokota, 1981). Such rapid pH change is not suitable for target benthic ecosystems. Fine grain oyster shells are therefore not suitable. Furthermore, very fine grain oyster shells become viscid and muddy when they are mixed together with coastal sediments. This is why crushed oyster shells with 7~12 mm pieces were selected.

The material was ground into powder using an agate mortar, and the powder X-ray diffraction patterns (XRD) were recorded by an XRD instrument (Rigaku-RINT1100K, Rigaku) using Cu K $\alpha$  radiation at 20 kV, 20

1 mA. Organic carbon, carbonate and nitrogen were also determined with a  
2 CHN analyzer (MT-5, Yanaco) after removing carbonate by acidifying with  
3 HCl (Yamamuro and Kayanne, 1995).

4 The specific surface area of the crushed oyster shell was determined by the  
5 Brunauer-Emmett-Teller method (nitrogen gas adsorption) using a  
6 Micromeritics adsorption equipment (Micromeritics Gemini 2370, Shimazu).

7 Scanning electron microscopic image was taken using a SEM (ABT-150F,  
8 TOPCON) at an accelerating voltage of 10 kV.

9 Wet degradation was carried out to determine the elements comprising the  
10 material. A 0.2 g powder sample was degraded at 100 °C on a hot plate with  
11 the addition of 5 mL ultra pure nitric acid in a Teflon beaker . After wet  
12 degradation, the sample was filtered through a 0.45 µm membrane filter (HA,  
13 Millipore). The elements in the filtrate were determined by ICP-AES  
14 (Optima3000, Perkin Elmer).

## 16 **2.2. Adsorption experiment**

### 17 **2.2.1. Removal kinetics**

18 Adsorption kinetics experiment was carried out in a 100 mL BOD bottle  
19 containing 50 mL of the hydrogen sulfide solution within the concentration  
20 range of 20~800 mg-S L. The hydrogen sulfide solution was prepared as  
21 follows: aliquot of Na<sub>2</sub>S·9H<sub>2</sub>O (Nacalai Tesque) was dissolved in 500 mL of a  
22 deaerated 3 % NaCl solution purged with N<sub>2</sub> gas. Thereafter, the pH of the  
23 solution was adjusted to 8.2 with 0.1 mol L<sup>-1</sup> HCl. 50 mL of hydrogen  
24 sulfide solution was slowly dispensed into the bottle and 1.0 g of the crushed  
25 oyster shell was added to the solution. The gas phase in the bottle was  
26 replaced with N<sub>2</sub> gas by blowing N<sub>2</sub> gas and capping the bottle tightly. The  
27 bottle was agitated moderately at 100 rpm at 25°C in a water bath and time

course of hydrogen sulfide concentration was monitored with a detection tube (200SB, Komyo Rikagaku Kougyo). A blank test in the absence of the crushed oyster shells were also conducted following the same procedure to compensate for hydrogen sulfide loss due to oxidation and volatilization, etc. These same settings were prepared in triplicates.

The adsorption kinetics of hydrogen sulfide onto the crushed oyster shell was calculated on the basis of equation (1).

$$q_t = \frac{\{(C_0 - C_t) - (C_{b0} - C_{bt})\}V}{W} \quad (1)$$

where  $q_t$  is the adsorbed hydrogen sulfide (mg-S g<sup>-1</sup> of the crushed oyster shell) at time  $t$ ,  $V$  is the volume of solution (L),  $C_t$  is the crushed oyster shell bottle (mg-S L<sup>-1</sup>) at time  $t$ ,  $C_0$  is the initial concentration.  $C_{bt}$  and  $C_{b0}$  are the concentrations of hydrogen sulfide in the blank (mg-S L<sup>-1</sup>) at time  $t$  and the initial concentration, respectively. The  $W$  is the amount of the crushed oyster shell used (g).

### 2.2.2. Adsorption isotherm

Hydrogen sulfide solution with a concentration range of 5~800 mg-S L<sup>-1</sup> was prepared following the same procedure described above. 50 mL of hydrogen sulfide solution was slowly dispensed into a 100 mL BOD bottle and 1.0 g of the crushed oyster shells were added to the solution with the head space in the bottle substituted with N<sub>2</sub> gas and the bottle was closed tightly. The bottle was agitated moderately at 100 rpm at 25°C in a water bath until achieving equilibrium (2~10 d) at which time hydrogen sulfide concentration was measured with a detection tube (200SB, Komyo Rikagaku Kougyo). The blank test in the absence of crushed oyster shells was also conducted

following the same procedure to compensate for hydrogen sulfide loss during the oxidation and volatilization. These same settings were prepared in triplicates.

The amount of hydrogen sulfide adsorbed onto the crushed oyster shell was calculated using equation (2).

$$q_e = \frac{\{(C_0 - C_e) - (C_{b0} - C_{be})\}V}{W} \quad (2)$$

where  $q_e$  is the hydrogen sulfide adsorbed (mg-S g<sup>-1</sup> of the crushed oyster shell) at equilibrium,  $V$  is the volume of solution (L),  $C_e$  is the concentration of hydrogen sulfide in the crushed oyster shell bottle (mg-S L<sup>-1</sup>) at equilibrium and  $C_0$  the initial concentration,  $C_{be}$  is the concentration of hydrogen sulfide in the blank at equilibrium (mg-S L<sup>-1</sup>) and  $C_{b0}$  the initial concentration, while  $W$  is the weight of the crushed oyster shell (g).

### 2.3. X-ray absorption fine structure (XAFS) of crushed oyster shell

The hydrogen sulfide adsorbed sample was prepared as follows: A 500 mg-S L<sup>-1</sup> hydrogen sulfide solution was prepared dissolving 1.9 mg of Na<sub>2</sub>S·9H<sub>2</sub>O (Nacalai Tesque) in 500 mL of deaerated Milli-Q water purged with N<sub>2</sub> gas, thereafter pH of the solution was adjusted to 8.2 with 0.1 mol L<sup>-1</sup> HCl. The 50 mL of 500 mg-S L<sup>-1</sup> hydrogen sulfide solution was slowly dispensed into a 100 mL BOD bottle and 1.0 g of the crushed oyster shell was added to the solution and head space in the bottle was substituted for N<sub>2</sub> gas and stopper of the bottle was closed tightly. Then, the bottle was agitated moderately at 100 rpm at 25°C in a water bath for 5 d. After the adsorption of hydrogen sulfide onto the crushed oyster shell, the sample was air-dried for 2

d in a dark place.

XAFS analysis was conducted using the BL11 of Hiroshima Synchrotron Research Center (Hayakawa et al., 2008). The synchrotron radiation from a bending magnet was monochromatized with a Si(111) double-crystal monochromator. The sample chamber was filled with He gas, and XAFS spectra were measured both by the X-ray fluorescence yield (XFY) mode and conversion electron yield (CEY) mode simultaneously. Energy of the incident X-rays was calibrated with the S K-edge XAFS spectrum of  $\text{CuSO}_4$  obtained with the CEY mode, and the main peak corresponding to the  $\text{SO}_4^{2-}$  was set to be 2.4816 keV according to the previous report (Backnaes et al., 2008). Pieces of relatively flat crushed oyster shell were measured without further treatment to conserve the surface condition of them. Each sample was mounted on a double-stick tape (NW-K15 ;Nichiban) placed in the central hole (15 mm in diameter) of a copper plate. The angle between the incident x-rays and the sample surface was 20 deg, and the X-ray fluorescence was detected from the direction normal to the incident beam in the plane of electron orbit of the storage ring. XAFS spectra were compared between crushed oyster shells with and without hydrogen sulfide treatment.

## **2.4. Container experiments**

### **2.4.1 Experimental settings**

The container experiment was designed for simulating enclosed water bodies and shown in Fig. 1. The crushed oyster shell and sediments (described below) were mixed in round-shaped black polyethylene containers ( $\phi$ : 550 mm, h: 420 mm), and sand-filtered natural seawater was supplied and allowed to overflow at an exchange rate of  $0.7 \text{ d}^{-1}$ , which is the average exchange rate of seawater between the upper and the lower layers of the

water column in the northern part of Hiroshima Bay. These containers were placed in a water bath (1000 L FRP container) to prevent rapid water temperature change during the experimental period. The light intensity was adjusted to 50~120  $\mu\text{mol m}^{-2} \text{s}^{-1}$  for simulating shallow coastal area conditions using loosely-woven nylon black sheets (cheese cloth) placed over the containers.

The sediment was collected from the Ohzu Inlet located at the head of Hiroshima Bay where municipal wastewater discharging is significant. Debris and pebbles were removed from the sediments before use. In the experimental container, 50 L of sediment and 50 L of the crushed oyster shell were mixed, while 50 L of sediment without the shells was used as a control. These settings were prepared in triplicates.

#### **2.4.2 Overlying seawater analyses**

Water temperature, salinity and pH were measured by a multiple electrode (U-10, Horiba). Dissolved oxygen concentration was determined by titration (Winkler method; APHA, 1989).

#### **2.4.3 Sediment and hydrogen sulfide in pore water analysis**

Sediment was collected with a container ( $\phi$ : 77 mm, h: 47 mm), and pH (PRN-40, Fujiwara) and ORP (RM-12P, TOA DK) were measured immediately thereafter. The container was then sealed and kept in a cool, dark place and transported to the laboratory. The sediment was centrifuged at 3,500 rpm for 10 min to separate pore water from the sediment and concentration of hydrogen sulfide in the pore water was determined with a detection tube (200SB, Komyo Rikagaku Kogyo).

### 3. Results and discussion

#### 3.1 Characterization of the crushed oyster shell

The chemical composition of the crushed oyster shell used in this study is shown in Table 1. The material was mainly composed of calcium carbonate. The concentrations of trace elements in this material were less than those in previous reports (Zn: 0.069~0.084 mg g<sup>-1</sup>, K: 0.08 mg g<sup>-1</sup>, Mn: 0.099~0.12 mg g<sup>-1</sup>, Fe: 0.07~0.39 mg g<sup>-1</sup>, Yokota, 1981, Yamada et al., 2003, Marine Blue 21, 2003). The specific surface area of the crushed oyster shell used in this study was 0.25 m<sup>2</sup> g<sup>-1</sup>, smaller than those of previous reports (1.75~9.59 m<sup>2</sup> g<sup>-1</sup>, Yoon et al., 2003; Park and Polprasert, 2008). The powder X-ray diffraction patterns showed the main crystal phase was calcite and CaO referring to a powder diffraction file (ICDD: 47-1743, JCPDS:28-775) (Fig. 3).

Oyster shells have two microstructural types within their shell structure: sheet phase layer and bulky phase layer (Yoon et al., 2003, Marine Blue 21, 2003). The sheet phase layers are composed of leaf shaped, hard, laminated layers. On the other hand, bulky phase layers are brittle and have a lot of pores with lattice-shaped structures.

The crushed oyster shells are classified into two products based on particle size. The coarse fraction which is mainly composed of sheet phase layer is used for feeds for chicken. The fine grain fraction which consisted of bulky phase layer is used for soil conditioners. The trace element contents in the fine grain fraction are higher than those of coarse fractions (Yokota, 1981). As shown in SEM image (Fig. 2), the crushed oyster shell with coarse grain used in this study is mainly composed of sheet phase layers.

The crushed oyster shell used in this study was coarse grain and its surface mainly consisted of sheet layer structures of calcite crystals and not bulky layers that are highly porous. Thus, the concentrations of trace elements in

the crushed oyster shell and its specific surface area used in this study were less than previous reports.

The calcite ( $\text{CaCO}_3$ ) to  $\text{CaO}$  transformation is verified at 500~600 °C and  $\text{CaCO}_3$  decomposition actively occurs at a temperature of around 810~850 °C (Balmain et al., 1999, Wilburn et al., 1991, Lee et al., 2008ab). Thus, the crushed oyster shell used in this study contains  $\text{CaO}$  initially, not derived from the drying process because drying temperature (400 °C) is lower than the transformation and decomposition temperature of  $\text{CaCO}_3$ .

## 3.2 Adsorption experiment

### 3.2.1 Removal kinetics

Removal kinetics of hydrogen sulfide under different initial concentrations is shown in Fig. 4. The concentrations of hydrogen sulfide decreased dramatically through time and its decreasing rate was expressed as first order equation described by equation (3). The first order rate constants and correlation coefficients between observed values and calculated values by the equation (3) are shown in Table 2.

$$[C_t] = [C_0]e^{-kt} \quad (3)$$

Where,  $[C_t]$  : concentration of hydrogen sulfide at time  $t$  (mg-S  $\text{L}^{-1}$ ),  $[C_0]$  : initial concentration of hydrogen sulfide (mg-S  $\text{L}^{-1}$ ),  $t$  : time (d), and  $k$  : first order rate constant ( $\text{d}^{-1}$ ).

### 3.2.2 Adsorption isotherm

Adsorption isotherm for hydrogen sulfide is shown in Fig. 5A. Here, three types of adsorption models, namely Langmuir model, Freundlich model and

Henry model, described by equations (4), (5) and (6), respectively, were applied to the hydrogen sulfide adsorption.

$$\frac{1}{q_e} = \frac{1}{ab} \cdot \frac{1}{C_e} + \frac{1}{a} \quad (4)$$

$$\log q_e = \log K_f + \frac{1}{n} \log C_e \quad (5)$$

$$q_e = HC_e \quad (6)$$

Where,  $q_e$ : the hydrogen sulfide adsorbed (mg-S g<sup>-1</sup>) at equilibrium,  $C_e$ : the concentration of hydrogen sulfide (mg-S L<sup>-1</sup>) at equilibrium,  $a$ : maximum adsorption capacity (mg-S g<sup>-1</sup>),  $b$ : adsorption coefficient related to bonding energy (L mg<sup>-1</sup>),  $H$ : Henry constant (L g<sup>-1</sup>),  $K_f$ ,  $n$ : Freundlich constant.

Both Freundlich model and Henry model were not suitable for hydrogen sulfide adsorption onto the crushed oyster shell because their correlation coefficients were low: 0.828 for Freundlich model and 0.803 for Henry model. On the other hand, Langmuir model fitted well (Fig. 5B). However, the adsorption equation was separated into two concentration ranges at equilibrium: less than 4.9 mg-S L<sup>-1</sup> and more than 4.9 mg-S L<sup>-1</sup>. The several parameters for hydrogen sulfide adsorption expressed as Langmuir model are shown Fig. 5B. The maximum adsorption capacity was 12 mg-S g<sup>-1</sup>. In this paper, the maximum adsorption capacity was compared with those of adsorbents for gaseous H<sub>2</sub>S because there is no report on maximum adsorption capacities of hydrogen sulfide in water. The maximum adsorption capacity was 2.3-71, 0.53-12.0, 14-1530 mg-S g<sup>-1</sup> for activated carbons, montmorillonites and an activated carbon catalyst (Guo et al., 2007, Xiao et al., 2008, Nguyen et al. 2005, Bashkova et al., 2007). The adsorption capacity of the crushed oyster shell was comparable to momorillonites and some

activated carbons.

### 3.3. X-ray absorption fine structure (XAFS) of crushed oyster shell

Sulfur K-edge XAFS spectra of crushed oyster shell were compared between those with and without hydrogen sulfide adsorbed (Fig. 6). The spectra were obtained with the XFY mode, and they were normalized with the XFY at the 2.490 keV. After the H<sub>2</sub>S adsorption a new peak appeared at 2.472 keV while the main peak corresponding to the sulfate (2.4816 keV) decreased. It was concluded that hydrogen sulfide was adsorbed onto the crushed oyster shell, and they were in the form of S<sup>2-</sup> (Fleet et al., 2005). The decrease of the sulfate peak may be attributed to the coverage of the adsorbed hydrogen sulfide. Since the outer surface of the crushed oyster shells is covered with hydrogen sulfide after adsorption treatment, the sulfate X-ray fluorescence signal seen after hydrogen sulfide adsorption becomes weaker than that prior to adsorption.

### 3.4 Container experiments

The water temperature, salinity and pH of overlying water changed in the range of 23.6~29.4°C, 2.85~3.13‰, 8.0~8.4, respectively, and did not show significant differences between the experiments and the control throughout the experimental periods. The concentrations of DO in the overlying water of the experimental containers were higher than that of the control after Day 25 with a statistical difference ( $p < 0.05$ ) on Day 35 (Fig. 7).

The pH of the sediment did not show a significant difference between the experiments and the control during the experimental periods, changing in the range of 6.7~7.8. The ORP of the sediment was more positive (-348~-252 mV) in the experiments than the control (-378~-349 mV), showing a

1 statistical difference ( $p < 0.01$ ) just after the addition of the materials. The  
2 concentration of hydrogen sulfide in the pore water was lower than the  
3 detection limit ( $< 0.1 \text{ mg-S L}^{-1}$ ) during the experimental period (Fig. 8). On  
4 the other hand, the hydrogen sulfide concentration of the control increased to  
5  $7.6 \text{ mg-S L}^{-1}$ .

6 From the results described above, the oyster shells apparently adsorbed  
7 hydrogen sulfide from pore water and formed  $\text{S}^0$ ,  $\text{S}_2\text{O}_3^{2-}$ ,  $\text{SO}_3^{2-}$  by oxidation of  
8 hydrogen sulfide as mentioned by Hayes and Taylor (2006). As a result, the  
9 DO concentration of overlying water and ORP of the sediment in the  
10 experiments were higher than those of the control (Fig. 7).

#### 12 4. Conclusions

13 The purposes of the present study include investigating adsorption  
14 characteristics of hydrogen sulfide onto crushed oyster shell, and to evaluate  
15 the removal efficiency of hydrogen sulfide from pore water in organically  
16 enriched sediments using container experiments. The results were as  
17 follows:

18 (1) The crushed oyster shell used in this study was mainly composed of  
19 calcium carbonate with calcite and CaO crystal phase. The specific surface  
20 area was  $0.25 \text{ m}^2 \text{ g}^{-1}$ .

21 (2) Removal kinetics of hydrogen sulfide was expressed as a first order  
22 equation. Langmuir model was fitted well to the hydrogen sulfide adsorption  
23 kinetics with an adsorption maximum at  $12 \text{ mg-S g}^{-1}$ .

24 (3) The container experiments showed that the oyster shell adsorbed  
25 hydrogen sulfide in pore water effectively and reduced oxygen consumption  
26 required for oxidation of hydrogen sulfide. As a result, the DO concentration  
27 of overlying water and ORP of the sediment in the experiments were higher

1 than those in the control.

2 Thus, it is concluded that the application of crushed oyster shells is effective  
3 in reducing hydrogen sulfide in the pore water of organically enriched  
4 sediments, which in turn may prevent DO depletion in the overlying water  
5 and decrease in ORP of sediments. The crushed oyster shell is one of the  
6 effective amendments to remediate organically enriched sediments in  
7 eutrophic coastal seas.

## 9 **Acknowledgements**

10 The authors thank Mr. Hitoshi Toda and Mr. Toshiyuki Ishizu of the  
11 Department of Agriculture, Forestry and Fisheries in Hiroshima City, and  
12 the staff of the Fisheries Promotion Center in Hiroshima for their kind  
13 assistance on container experiments. We are grateful to Shiroh Kobayashi  
14 (MARUEI Corporation) for his helpful comments about crushed oyster shell.  
15 Experiments at HiSOR were carried out under the approval of the HSRC  
16 Program Advisory Committee (#:08-A-34). We also thank Professor Masaki  
17 Taniguchi for the approval of the HSRC program. This work was partly  
18 supported by the “Research for Community Contribution” project provided  
19 by Hiroshima University.

## 21 **References**

22 American Public Health Association, American Water Works Association,  
23 Water Pollution Control Federation, 1989. Standard method for  
24 examination of water and wastewater., 17th ed. APHA, Washington DC.  
25 Backnaes, L., Stelling, J., Behrens, H., Goettlicher, J., Mangold, S., Verheijen,  
26 O., Beerkens, R. G. C., Deubener, J., 2008. Dissolution mechanisms of  
27 tetravalent sulphur in silicate metals: evidence from sulphur K edge

1 XANES studies on glasses. J. Am. Ceram. Soc. 91, 721-727.

2 Balmain, J., Hannoyer, B., Lopez, E., 1999. Fourier transform infrared  
3 spectroscopy (FTIR) and X-ray diffraction analyses of mineral and  
4 organic matrix during heating of mother of pearl (nacre) from the shell of  
5 the mollusk *Pinctada maxima*. J. Biomed. Mater. Res. B(Appl. Biomater.)  
6 48, 749-754.

7 Bashkova S., Baker F. S., Wu X., Armstrong T. R., Schwartz V., 2007.  
8 Activated carbon catalyst for selective oxidation of hydrogen sulphide: On  
9 the influence of pore structure, surface characteristics, and  
10 catalytically-active nitrogen. Carbon. 45, 1354-1363.

11 Fleet, M. E., Harmer, S. L., Liu, X., Nesbitt, H. W., 2005. Polarized X-ray  
12 adsorption spectroscopy and XPS of TiS<sub>3</sub>; S K-and Ti L-edge XANES and  
13 S and Ti 2p XPS. Surf. Sci. 584, 133-145.

14 Guo, J., Luo, Y., Lua, A. C., Chi, R., Chen, Y., Bao, X., Xiang, S., 2007.  
15 Adsorption of hydrogen sulphide (H<sub>2</sub>S) by activated carbons derived from  
16 oil-palm shell. Carbon. 45, 330-336.

17 Hayakawa, S., Hajima Y., Qiao, S., Namatame, H., Hirokawa, T., 2008.  
18 Characterization of calcium carbonate polymorphs with Ca K edge X-ray  
19 adsorption fine structure spectroscopy. Anal. Sci. 24, 835-837.

20 Hayes, M. K., Taylor, G. T., 2006. Vertical distributions of thiosulfate and  
21 sulfite in the Cariaco Basin. Limnol. Oceanogr. 51, 280-287.

22 ICDD- International Center for Diffraction Data (1997) Powder diffraction  
23 file set 47. International Center for Diffraction Data, 47-1743.

24 JCPDS-International Centre for Diffraction Data (1986) Powder diffraction  
25 file sets 27 to 28. International Center for Diffraction data, 27-775.

26 Lee, C. H., Lee, D. K, Alia, M. A., Kima, P. J., 2008a. Effects of oyster shell on  
27 soil chemical and biological properties and cabbage productivity as a

liming materials. Waste Manage. 28, 2702-2708.

Lee, S. W., Kim, Y. M., Kim, R. H., Choi C. S., 2008b. Nano-structured biogenic calcite: A thermal and chemical approach to folia in oyster shell. Micron 39, 380-386.

Marine Blue 21, 2003. Introduction to livestock waste water treatment system by utilization of shells, Marine Blue 21, Tokyo, pp.13-18. (in Japanese)

Ministry of Agriculture, Forestry and Fisheries of Japan., 2007. <http://www.maff.go.jp/toukei/sokuhou/data/gyogyou-yousyoku2007/gyogyou-yousyoku2007.pdf>, (accessed on 17 Feb. 2009)

Nakatani, N., Takamori, H., Takeda, K., Sakugawa, H., 2009. Transesterification of soybean oil using combusted oyster shell waste as a catalyst. Biores. Technol. 100, 1510-1513.

Nguyen-Thanh, D., Block, K., Bandosz, T. J., 2005. Adsorption of hydrogen sulfide on montmorillonites modified with iron. Chemosphere. 59, 343-353.

Park, W. H., Polprasert, C., 2008. Roles of oyster shells in an integrated constructed wetland system designed for P removal. Ecol. Eng. 34, 50-56.

Wilburn, F. W., Sharp, J. H., Tinsley, D. M., McIntosh, R. M., 1991. The effect of procedural variables on TG, DTG and DTA curves of calcium carbonate. J. Therm. Anal. 37, 2003-2019.

Xiao Y., Wang S., Wu, D., Yuan, Q., 2008. Experimental and simulation study of hydrogen sulfide adsorption on impregnated activated carbon under anaerobic conditions. J. Hazard. Mater. 153, 1193-1200.

Yamada M., Taniguchi K., Okumura M., Sano H., 2003. Deflection properties of pavement constructed on subgrade containing crushed oyster shell. J. Soc. Mater. Sci. Japan 53, 25-28. (in Japanese with English abstract)

- 1 Yamamuro, M., Kayanne, H., 1995. Rapid direct determination of organic  
2 carbon and nitrogen in carbonate-bearing sediments with a Yanaco MT-5  
3 CHN analyzer. *Limnol. Oceanogr.* 40, 1001-1005.
- 4 Yokota H., 1981. Edaphological studies on the utilization of the oyster shells.  
5 *Bull. Hiroshima Agric. Coll.* 6, 549-639. (in Japanese with English  
6 abstract)
- 7 Yoon, G. L., Kim, B. T., Kim, B. O., Han, S. H. , 2003. Chemical–mechanical  
8 characteristics of crushed oyster-shell. *Waste Managem.* 23, 825-834.

Table 1 Chemical composition of the crushed oyster shell used in this study  
(mg g<sup>-1</sup>)

Table 2 Removal rate constant for hydrogen sulfide expressed as first order  
equation

Fig.1. Schematic drawing of the container experimental setting

Fig. 2 SEM image of the crushed oyster shell

Fig. 3 X-ray diffraction pattern of the crushed oyster shell

Fig.4 Removal kinetics of hydrogen sulfide under different initial  
concentrations with crushed oyster shell

Fig. 5 Adsorption isotherm (A) and Langmuir plots (B) for hydrogen sulfide  
onto the crushed oyster shell

Fig. 6 Sulfur XAFS spectrum of crushed oyster shell with and without  
hydrogen sulfide adsorbed by X ray fluorescence yield method

Fig. 7 Change in DO concentrations of overlying water

Fig. 8 Change in hydrogen sulfide concentrations in pore water

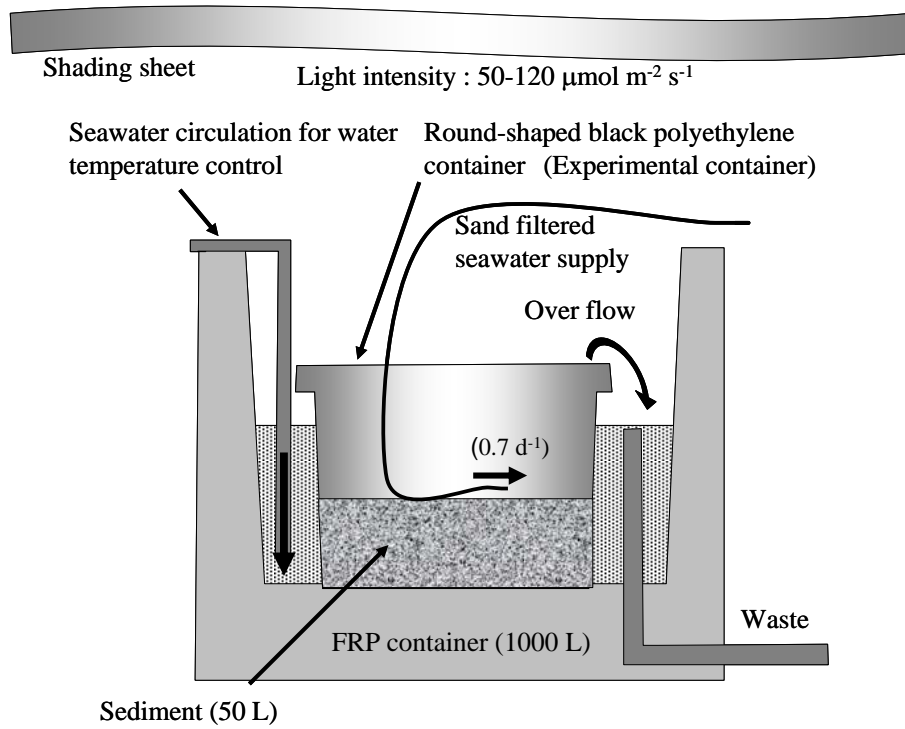


Fig.1.

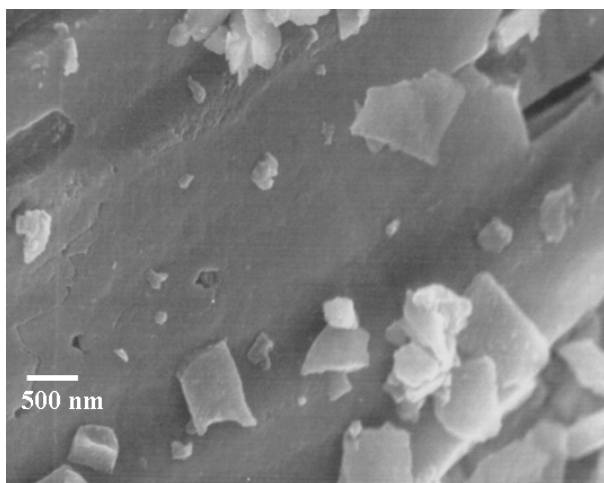


Fig. 2

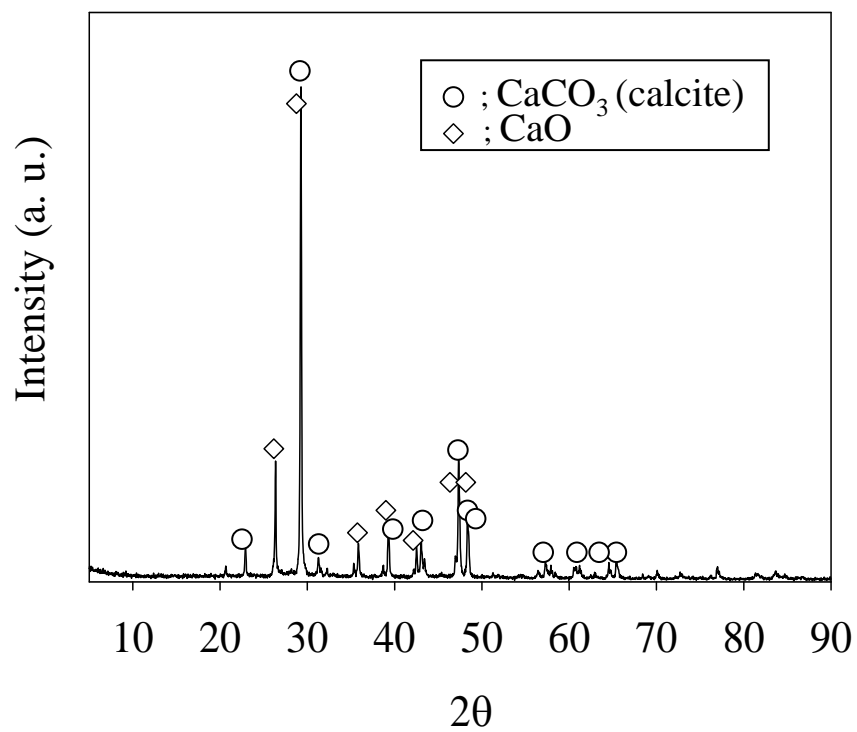


Fig. 3

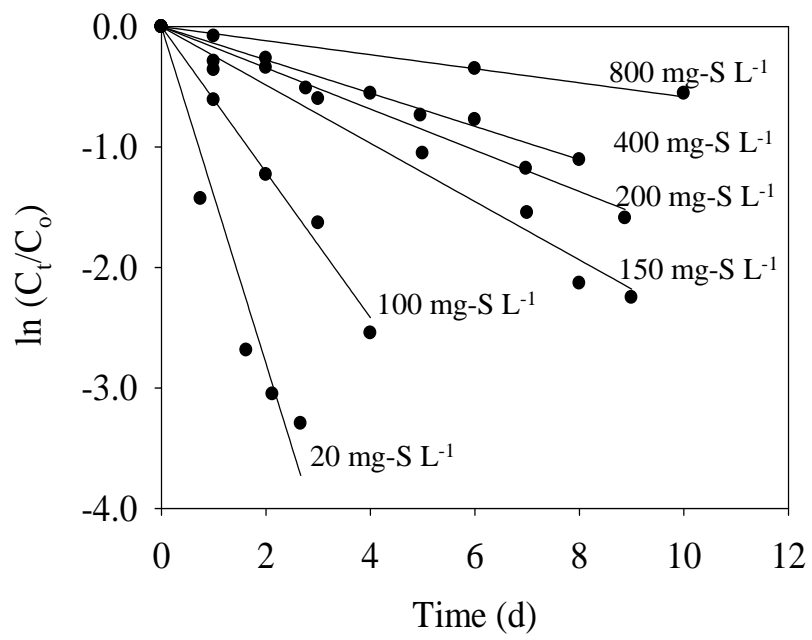


Fig.4

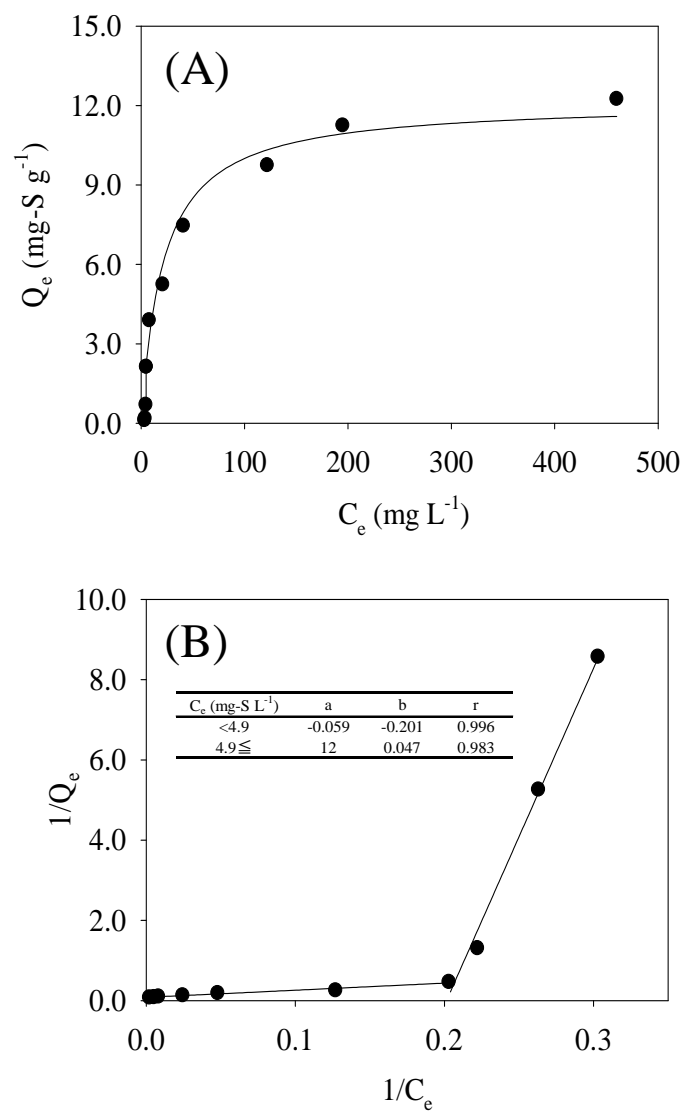


Fig. 5

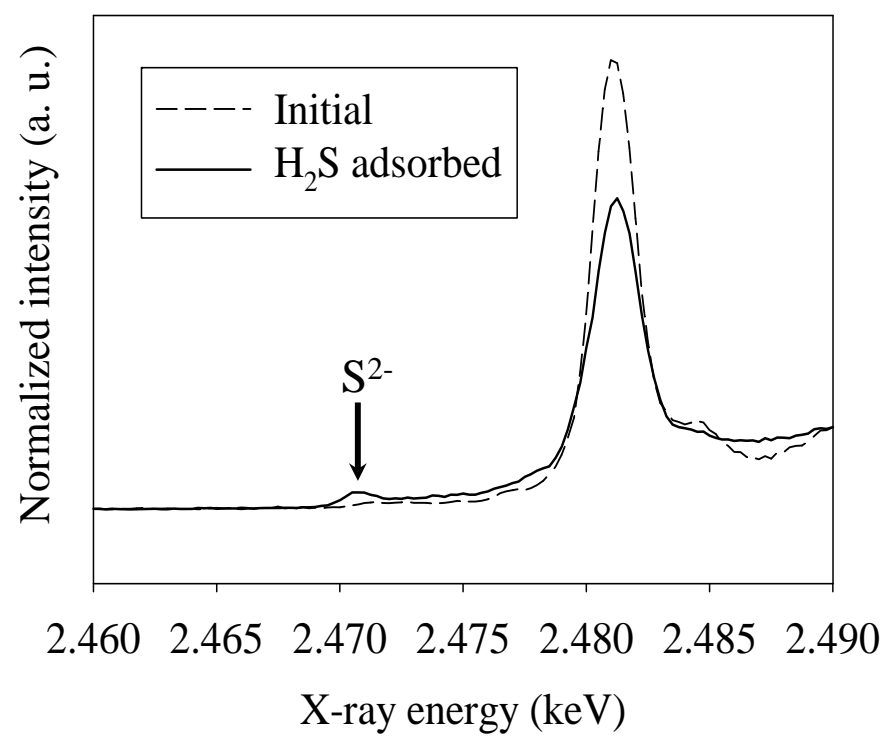


Fig. 6

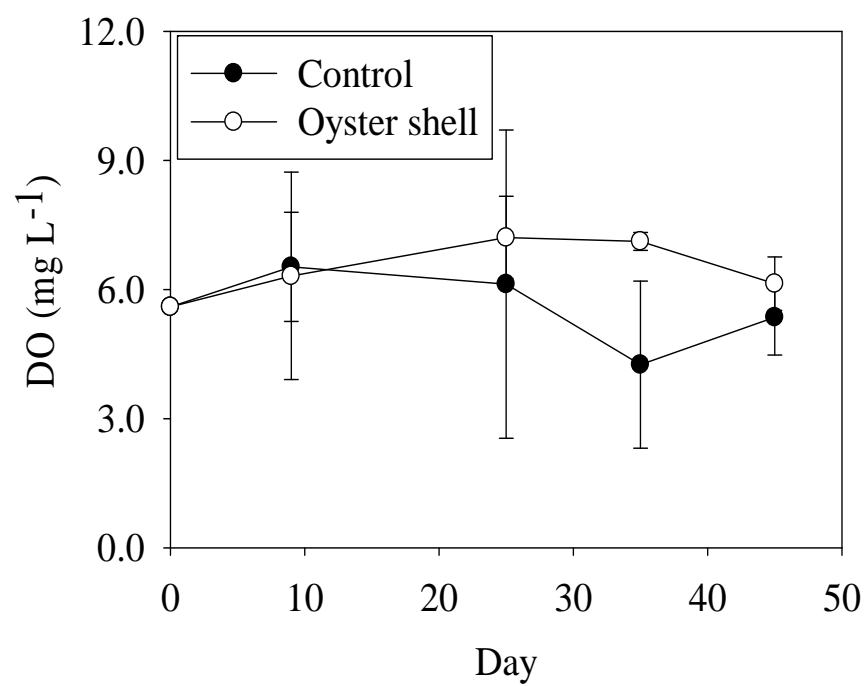


Fig. 7

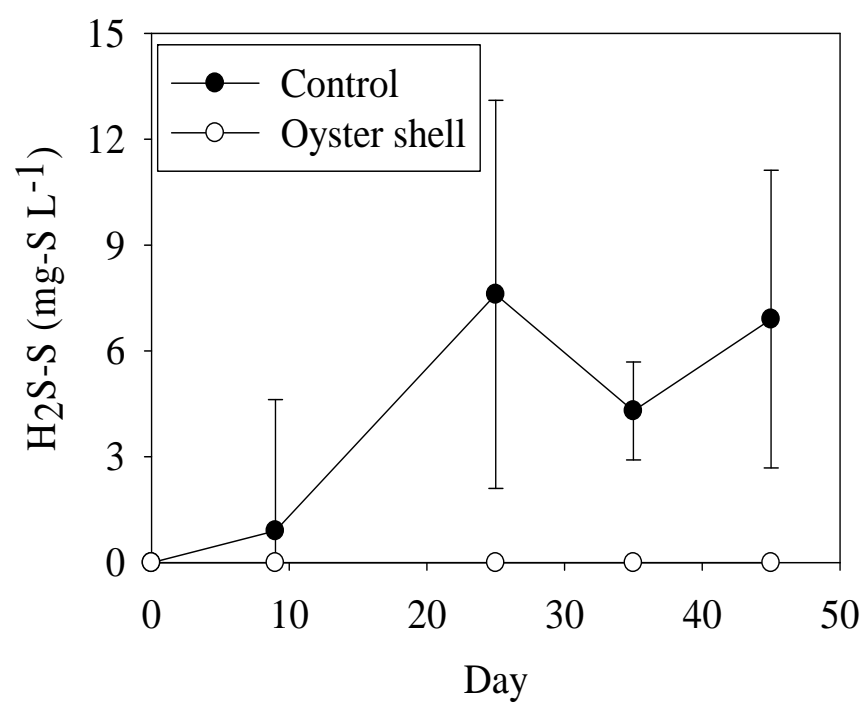


Fig. 8

Table 1

CO <sub>3</sub>	569	Sr	0.43
Ca	404	Zn	0.03
C	19.9	K	0.02
Na	4.1	Mn	0.02
N	1.8	Fe	0.009
Mg	0.94		

Table 2

Initial concentration (mg-S L <sup>-1</sup> )	<i>k</i> (d <sup>-1</sup> )	r
20	1.4	0.961
100	0.60	0.993
150	0.24	0.987
200	0.17	0.993
400	0.14	0.980
800	0.058	0.940